electrochem

MDPI

Article

Full Tailored Metal Content NCM Regeneration from Spent Lithium-Ion Battery Mixture Under Mild Condition

Alpha Chi Him Tsang [1], Shaobo Ouyang [2,*], Yang Lv [3], Chi Chung Lee [4], Chi-Wing Tsang [1] and Xiao-Ying Lu [1,*]

[1] Department of Construction, Environment and Engineering, Technological and Higher Education Institute of Hong Kong, Tsing Yi, Hong Kong, China
[2] Faculty of Material Metallurgy and Chemistry, Jiangxi University of Science and Technology, Ganzhou 341000, China
[3] School of Civil Engineering, Dalian University of Technology, Dalian 116024, China
[4] School of Science and Technology, Hong Kong Metropolitan University, Hong Kong, China; cclee@hkmu.edu.hk
* Correspondence: ouyangshaobo2@163.com (S.O.); xylu@thei.edu.hk (X.-Y.L.)

Abstract: Mild conditioned, second-life ternary nickel–cobalt–manganese (NCM) black powder regeneration from spent lithium-ion batteries' (LIBs) black powder mixture was demonstrated after mild conditioned p-toluenesulphuric acid (PTA)-assisted wet leaching. The NCM ratio was tailored to several combinations (333, 523, 532, and 622) by adding a suitable amount of metal (Ni, Co, Mn)-sulphate salt to the leachate. Regenerated NCM was obtained by co-precipitation with sodium hydroxide pellets and ammonia pH buffering solution, followed by lithium (Li) sintering under ambient air and size sieving. The obtained regenerated NCM powder was used for the energy storage materials (ESM) in coin cell (Li half-cell, CR2032) evaluation. Systematic characterization of regenerated NCM showed that the NCM ratio was close to the target value as assigned in the tailored process, and regenerated 622 (R622) exhibited strong activity in CR2032 coin cell testing among all four ratios with a maximum discharge capacity of 196.6 mAh/g.

Keywords: organic acid; nickel–cobalt–manganese (NCM); spent lithium-ion batteries (LIBs); regeneration; coin cell

Citation: Tsang, A.C.H.; Ouyang, S.; Lv, Y.; Lee, C.C.; Tsang, C.-W.; Lu, X.-Y. Full Tailored Metal Content NCM Regeneration from Spent Lithium-Ion Battery Mixture Under Mild Condition. *Electrochem* **2024**, *5*, 546–559. https://doi.org/10.3390/electrochem5040035

Academic Editor: Masato Sone

Received: 10 October 2024
Revised: 8 November 2024
Accepted: 13 November 2024
Published: 2 December 2024

1. Introduction

Lithium-ion batteries (LIBs) are increasingly recognized as a green energy solution in modern society, particularly in response to the energy crisis stemming from the overconsumption of fossil fuels and the associated pollution. Their popularity can be attributed to several key advantages: they are rechargeable from external power sources, have a long service life, and provide high power output. These features have made LIBs particularly popular in the automotive industry (notably in electric vehicles (EVs)) and in portable devices such as laptops and mobile phones since 2009. However, the improper disposal of spent LIBs from used EVs, laptops, and mobile phones poses significant environmental risks, including water and land pollution. Spent LIBs often contain NCM black powder, which is composed of toxic heavy metals, organic electrolytes, and polymer separators. When disposed of as regular waste or inadequately treated in recycling facilities, these substances can be released into the environment, leading to severe pollution issues [1–4]. The volume of spent LIBs is projected to increase dramatically, reaching approximately 1 million tons by 2025 [3], 11 million tons by 2030 [1], and potentially 21 million tons by 2045 [5]. Improper disposal and treatment of exhausted LIBs can also result in fire hazards, endangering the lives of nearby residents and ecosystems [6–10]. Another critical issue is the waste of non-renewable natural resources. The ternary NCM black powder used in LIBs is manufactured from valuable d-block metals, including nickel (Ni), cobalt (Co),

and manganese (Mn), sourced from ore, as well as lithium (Li), extracted from freshwater systems (lakes, groundwater) and soil [2,4,6,7,9–12]. The high demand for LIBs, projected to continue through 2035, may lead to over-mining of these metal ores and result in underground water pollution. This demand is also likely to increase metal prices in the market. To mitigate the adverse effects of over-mining and improper disposal of spent LIBs, recycling spent batteries with proper treatment is essential. Developing technologies for the recycling of metals and energy storage materials (ESMs) is a critical step towards achieving solid waste reduction, effective recycling of non-renewable resources, and sustainable LIB manufacturing. This approach is vital for fostering a circular economy and minimizing environmental impact [7,8,13].

Synthesizing second-life NCM powder from spent LIB black powder by chemical regeneration involves three steps: (1) second-life NCM precursor synthesis; (2) co-precipitation; and (3) lithiation. Up-to-date, NCM ratio adjustment can be achieved by two methods. The first method involves the addition of specific metal salts (e.g., nickel (II) sulphate ($NiSO_4$), cobalt (II) sulphate ($CoSO_4$), manganese (II) sulphate ($MnSO_4$)) to the leachate obtained from hydrometallurgically treated spent LIB black powder [1,2,4,5,8,9,12,14]. Another method involves regenerating recovered NCM leachate from spent LIB black powder without adjusting the NCM ratio [3,11,15–19]. NCM precursors obtained from the above-mentioned methods are co-precipitated into the NCM hydroxide precursor by precipitating agents (e.g., sodium hydroxide) after adjusting the pH of the precursor solution. This step is crucial for ensuring that the necessary stoichiometry and phase are achieved in the final product. Regenerated NCM is produced through a lithiation process using external lithium sources (e.g., lithium carbonate (Li_2CO_3), lithium hydroxide/lithium nitrate mixture ($LiOH/LiNO_3$)) at high temperature in a furnace [2,3,5,8,9,18,19]. The above-mentioned NCM ratio tailoring can be achieved either by high-temperature [2,9] or room-temperature [1,5,8] solvation of the metal salts. Room-temperature tailoring is regarded as an environmentally friendly process due to the low input energy required. Tailored NCM regeneration to the designated NCM ratio only has been widely studied [2–5,8,9,11,12,14–19] up to the present, while there is a relative scarcity of studies that address the regeneration of various NCM ratios [1]. This focus may limit the applicability of the findings to real-world scenarios, where a mix of spent LIBs with varying NCM contents are processed.

In terms of the implications for industry, modern research predominantly uses single types of spent batteries, which may not reflect the conditions in industrial recycling facilities where mixed battery types are processed. As a result, developing suitable regeneration processes that can handle various spent LIBs efficiently and with minimal chemical and energy inputs is critical for advancing large-scale recycling.

In this study, we demonstrated a simple and environmentally friendly method for regenerating nickel–cobalt–manganese (NCM) materials. This process involved tailoring the NCM ratio from acidic leachate during the recovery of black powder from multiple spent lithium-ion batteries (LIBs) at room temperature and under non-inert gas conditions. We evaluated the electrochemical activity of the regenerated NCM by testing it in CR2032 coin cells (lithium half-cells) to assess the effectiveness of the regeneration process.

2. Materials and Methods

2.1. Materials

Sodium sulphate (Na_2SO_4) (99.9%, Sigma Aldrich 238597, Hong Kong, China), table salt (sodium chloride: NaCl), p-toluenesulphonic acid (PTA) (99%, Sigma Aldrich 402885, Hong Kong, China), hydrogen peroxide (H_2O_2) (30% v/v, Sigma Aldrich 216763, Hong Kong, China), nickel (II) sulphate hexahydrate ($NiSO_4 \cdot 6H_2O$) (99.99%, Sigma Aldrich 467901, Hong Kong, China), cobalt (II) sulphate heptahydrate ($CoSO_4 \cdot 7H_2O$) (99.99%, Sigma Aldrich 935751, Hong Kong, China), manganese (II) sulphate monohydrate ($MnSO_4 \cdot H_2O$) (99.99%, Sigma Aldrich M7634, Hong Kong, China), ammonia solution (NH_3) (30%, Sigma Aldrich 338818, Hong Kong, China), sodium hydroxide (NaOH) (98%, Sigma Aldrich S5881, Hong Kong, China), lithium carbonate (Li_2CO_3) (99.9%, Sigma Aldrich 255823, Hong

Kong, China), Al foil, N-methyl-2-pyrrolidone (NMP, Sigma Aldrich 443778, Hong Kong, China), SuperP (99+%, Thermo Scientific Chemicals 15457755, Loughborough, UK), poly (vinylidene difluoride) (PVDF, Sigma Aldrich 182702, Hong Kong, China), and lithium hexafluorophosphate ($LiPF_6$, Sigma Aldrich 746711, Hong Kong, China) electrolyte were used directly as purchased. PVDF gel for the cathode slurry was prepared by dissolving PVDF powder into NMP in a 1:9 w/w ratio with overnight stirring until the clear gel formed.

2.2. Metal Recovery from LIB Black Powder

2.2.1. Black Powder Extraction

Cathode black powder extraction involved two steps: (1) cathode sheet extraction and (2) powder extraction. In the first step, spent commercial LIBs were scraped to extract the cathode sheets. Two types of LIBs were used in this study, namely lithium manganese oxide (LMO) (battery A) and Ni-rich (battery B) LIBs. Briefly, the spent LIBs were discharged by soaking the batteries in brine water (Na_2SO_4 or NaCl), followed by manual scraping to obtain the cathode sheets. The cathode sheets were then cleaned by soaking in DI water overnight, followed by overnight drying in an oven (60 °C). The flow of scraping the spent LIBs to extracting the cathode sheets is summarized in Figure S1.

In the second step, the cleaned, dry cathode sheets were cut into several small sheets and calcinated in a furnace at 600 °C for 6 h initially in order to remove all the conductive binder (PVDF), followed by manual peeling of the black powder. The black powder collected was transferred to the ceramic pot for the second calcination in an oven at 600 °C for 6 h once again to ensure the complete removal of residual PVDF from the extracted powder.

2.2.2. Hydrometallurgy Driven Metal Recovery

Metal recovery in the current study was achieved by modified, strong organic acid ($pK_a < 0$)-assisted leaching at low temperature [20]. Briefly, 4 g black powder mixture was added to a 50 mL PTA (2M) and H_2O_2 (9%) binary solution (PTA/H_2O_2 = 3:7 (v/v)) in order to form a 80 g/L plug ratio (solid/liquid) dispersion. The mixture was heated at 70 °C with constant stirring for 2h in a 250 mL three-necked, round-bottom flask. The leachate collected was filtered through a nylon-filter-equipped syringe (10 mL) to remove all solid particulates before proceeding to Inductively Coupled Plasma Optical Emission Spectrometry (ICP-OES) analysis and NCM regeneration. Filtered leachate from multiple spent LIBs (two types) was mixed into a single stock in a 1:1 v/v ratio, and the corresponding composition is summarized in Table S1. Figure S2 summarizes the full process of black powder calcination and PTA-assisted acid leaching.

2.2.3. Material Characterisation

Metal ion concentration in the fresh and metal-adjusted leachate for co-precipitation was analyzed by Inductively Coupled Plasma Optical Emission Spectroscopy (Agilent-5110 ICP-OES, Agilent, Santa Clara, CA, USA). The morphology of regenerated NCM powder was characterized by SEM (LEO-1350 FE-SEM, Zeiss, Oberkochen, Germany). Its crystal structure was analyzed by XRD (Philips X-Perts', Amsterdam, Holland: Cu-Kα radiation; accelerating voltage: 40 kV; current: 20 mA; scan range (2θ): 10–80°; the sample powder was ground into fine powder by the gravity grinder prior to analysis). Its chemical composition (elemental information and composition) was analyzed by XPS (Physical Electronics PHI 5802, Eden Prairie, MN, USA: C1s signal at 285 eV was used to make the appropriate charging effect corrections) and EDS (equipped in LEO-1350), respectively.

2.3. Ternary NCM Black Powder Regeneration and Battery Performace Testing

2.3.1. Ternary NCM Powder Regeneration

Regeneration of ternary NCM from PTA-assisted leaching was carried out by modifying the process from another report [1]. Briefly, a suitable amount of metal sulphate salts (Ni (II), Co (II), and Mn (II)) was added to the desired amount of acidic leachate mixture

stock solution (30 mL) for NCM content adjustment. ICP-OES was carried out to monitor the NCM ratio of the leachate stock in every adjustment until it reached the designated value (i.e., 333, 523, 532, 622). Metal-content-adjusted leachate was neutralized to pH ~7 by 30% NH_3, followed by complete co-precipitation of metal ions by adding a suitable amount of NaOH pellets to the solution at controlled pH (<11) until the coloured solution turned colourless with precipitate scum formed after overnight settling. Precipitate was obtained by centrifugating the dispersion, followed by cleaning the sediments with DI water several times and drying overnight (60 °C, 48 h). The final NCM product was synthesized by mixing dried precipitate with the desired amount of Li_2CO_3 (1.1 times in excess of the number of moles of the NCM hydroxide precursor) according to the chemical Equation (1), followed by single-round sintering in a 2-step calcination programme (first step: 450 °C, 2 h; second step: 900 °C, 12 h). The regenerated NCM powder was cooled down to room temperature, followed by mechanical grinding and sieving (250-mesh pore).

$$Li_2CO_3 + 2Ni_xCo_yMn_z(OH)_2 + ½O_2 \rightarrow 2Li(Ni_xCo_yMn_z)O_2 + CO_2 + 2H_2O \quad (1)$$

2.3.2. Regenerated Battery Assembly

The regenerated NCM battery was fabricated by the following process. Briefly, active materials (regenerated NCM, conductive carbon (SuperP), PVDF gel; mass ratio = 8:1:1) in the above-mentioned sequence were mixed together in the NMP solvent to form a mixture with a solid (total solid)/liquid (total NMP) mass ratio of 3:7. The mixture was shaken for at least 15 min until liquid slurry formed. The slurry was deposited on the rear side of the Al foil (current collector) to form a 0.1 mm thin film, followed by overnight drying in a vacuum oven at 105 °C in order to remove the NMP solvent and preserving sample. A dried, regenerated NCM cathode sheet was then punched into a 12 mm disc, followed by pressing into a 10 μm thin film electrode in an oil-jet presser. The punched cathode disc was further dried in the same environment (105 °C, vacuum, overnight) before the CR2032 coin battery (Li half-cell) assembly in a glove box. The resulting mass loading of the regenerated NCM cathode, summarized in Table S2, lay in the range of 1.06–1.55 mg/cm^2. The Li block disc (12 mm), Celgard-2400 membrane (16 nm), and regenerated NCM disc (12 mm) acted as counter electrode, separator, and cathode respectively. The Li block disc placed inside the anode suitcase was wetted with the $LiPF_6$ electrode (3 drops on convex side) first, followed by placing the Celgard-2400 membrane and the regenerated NCM electrode disc sequentially. Finally, the coin battery was covered by the cathode suitcase. The as-assembled CR2032 coin battery was then packed by mechanical pressing in the oil-jet presser, followed by drying with Kimwisp paper to remove residual electrolyte on the battery surface. The flow diagram showing the regenerated NCM coin cell assembly is summarized in Figure 1.

2.3.3. Battery Performance Testing

Regenerated NCM battery performance was analyzed by a battery test system (LAND CT2001A, China; Software: LAND Battery Testing System-Ver 7.3) in glavanostatic cycling mode at a 0.1 C scan rate. The charging and discharging current was set at 0.015 mA with a voltage window of 3.0–4.2 V vs. Li^+/Li, and the total number of charging/discharging cycles was 51. The first cycle was defined at the second cycle of operation after coin cell activation (first operational cycle) in performance testing.

Figure 1. Flow of NCM regeneration and CR2032 coin cell assembly with coin cell components: 1: anode cap; 2: spring; 3: spacer; 4: Li block; 5: Celgard 2400 separator (Shenzhen, China) (wet with $LiPF_6$); 6: cathode disc; 7 cathode cap.

3. Results and Discussion

3.1. Material Characteristics of Regenerated NCM

The PTA-assisted valuable metals recovery from various spent LIBs under mild conditions (60 °C, 2 h) and a high plug ratio (S/L = 80 g/L) was effective, which was reflected by the close NCM ratio obtained from comparing the metal composition (Ni, Co, and Mn) of leachate from PTA leaching (ICP-OES) with that of extracted black powder from as-discharged spent LIBs (EDS), as summarized in Table S1. Furthermore, the raw waste belonged to the LMO (battery A) and Ni-rich NCM LIBs (battery B), according to the ICP-OES and EDS results of the raw leachate stock and black powder as listed in Table S1. Most importantly, the PTA used in the current work was a relatively green leaching agent compared with common mineral acids, which could prevent potential secondary pollution due to no toxic gas (sulphur dioxide (SO_2)) being generated by the PTA. This property is important when developing industrial-scale, low-emission NCM regeneration.

Regenerated second-life NCM samples obtained in the current study showed that NCM ratio tailoring can be achieved by adjusting the metal content in the leachate, where a different combination of NCM (333, 523, 532 and 622) was produced after co-precipitation of the NCM-adjusted leachate. The regenerated samples were named R333, R523, R532,

and R622, according to the EDS analysis of regenerated NCM, which is summarized in Table 1. Morphological analysis by a SEM method with images, which are depicted in Figure 2, showed that the roughly shaped primary particles were stacked into larger secondary particles throughout regeneration. The degree of particle stacking increased when the resulting NCM ratio increased, due to more metal ions being needed to achieve the tailoring, which resulted in a higher chance of metal ion aggregation during the co-precipitation. Furthermore, the primary particle size of different regenerated NCM products was approximately 225–525 nm, according to SEM images (Figure 2). The secondary particle size was analyzed by the particle size distribution (PSD) method. The results are summarized in Table 1, and Figure 3 shows that the regenerated NCM particle size distribution (D_{90}) lies in the range of 14.7–18.3 µm, with the exceptional case of R622 (61.8 µm). The exceptionally large secondary particle size recorded in R622 may have resulted from the strong aggregation of metal ions throughout the co-precipitation process in the regeneration of R622, due to the relatively large amount of Ni^{2+} being added in the leachate when compared with other regenerated NCM (R333, R523, R532). To date, some regenerated NCM samples have contained a secondary particle size range (D_{90}) as small as 3–5 to 19.2 µm [3,5,9] (D_{90} < 20 µm) to as large as 43–58 µm [21] (D_{90} > 40 µm), which was independent of the NCM ratio in the regenerated samples (e.g., 333 [3,5,21], 622 [9]). Such findings show that the random particle size was caused by multiple ion aggregation throughout co-precipitation in the regeneration process [21]. Secondary particle size of regenerated NCM samples in the current study (Table 1) lay in the range of the reported sample and had similar secondary particle size distribution, independent of the corresponding NCM ratio [3,5,9,21]. The results above show that the NCM ratio can be tailored easily by adjusting the metal content with fresh metal salts according to the ICP and EDS analysis (Table S1). At the same time, the current method has the advantage of achieving complete metal ion co-precipitation in the minimum solution volume via direct addition of NaOH pellets to the leachate solution.

Table 1. Composition of the regenerated NCM (at%) and corresponding PSD (D_{90}).

Sample	Ni (at%)	Co (at%)	Mn (at%)	NCM Composition	Particle Size (D_{90}) (µm)
R333	20.0	20.2	18.2	$Ni_{1.10}Co_{1.11}Mn_1$	14.8
R523	28.9	10.9	14.4	$Ni_{5.30}Co_2Mn_{2.64}$	18.3
R532	22.5	15.1	9.5	$Ni_{4.74}Co_{3.18}Mn_2$	14.7
R622	43.5	14.9	10.3	$Ni_{6.12}Co_2Mn_{1.46}$	61.8

The crystal structure of regenerated NCM samples was analyzed using X-ray diffraction (XRD), as summarized in Figure 4. All of them showed the α-$NaFeO_2$ layer structure with space group: R-3m (JCPDS no. 09-0063) compared with the XRD pattern of similar samples reported elsewhere [18,19,22–24]. The four sharp peaks observed at 2θ values of 18.8°, 36.8°, and 44.6° correspond to the (003), (101), and (104) planes, respectively. Additionally, clear splitting of the peaks at (006)/(012) and (018)/(110) was noted in the XRD pattern of the regenerated NCM (Figure 4), indicating a consistent structure irrespective of the final NCM ratios of the samples. This pattern is comparable with those reported for NCM samples with similar ratios in previous studies [18,19,22–24]. Moreover, the intensity ratio of the (003) to (104) peaks for the regenerated NCM range from 1.29 to 2.23 (>1.2), suggesting that the samples exhibited a highly crystalline structure with a low degree of cation mixing, as noted in earlier research [18,19,22–24]. The presence of peaks at 22.5° and 28.8° in R523 (Figure 4b) can be attributed to Li_2CO_3 and is matched by similar regenerated materials reported elsewhere [4]. It represents the presence of trace amounts of residual Li_2CO_3 throughout regeneration. In general, the overall results indicate that tailored regeneration of NCM can be effectively achieved by adjusting the amounts of Ni, Co, and Mn salts in the acidic leachates, alongside meticulous quality control through ICP-OES.

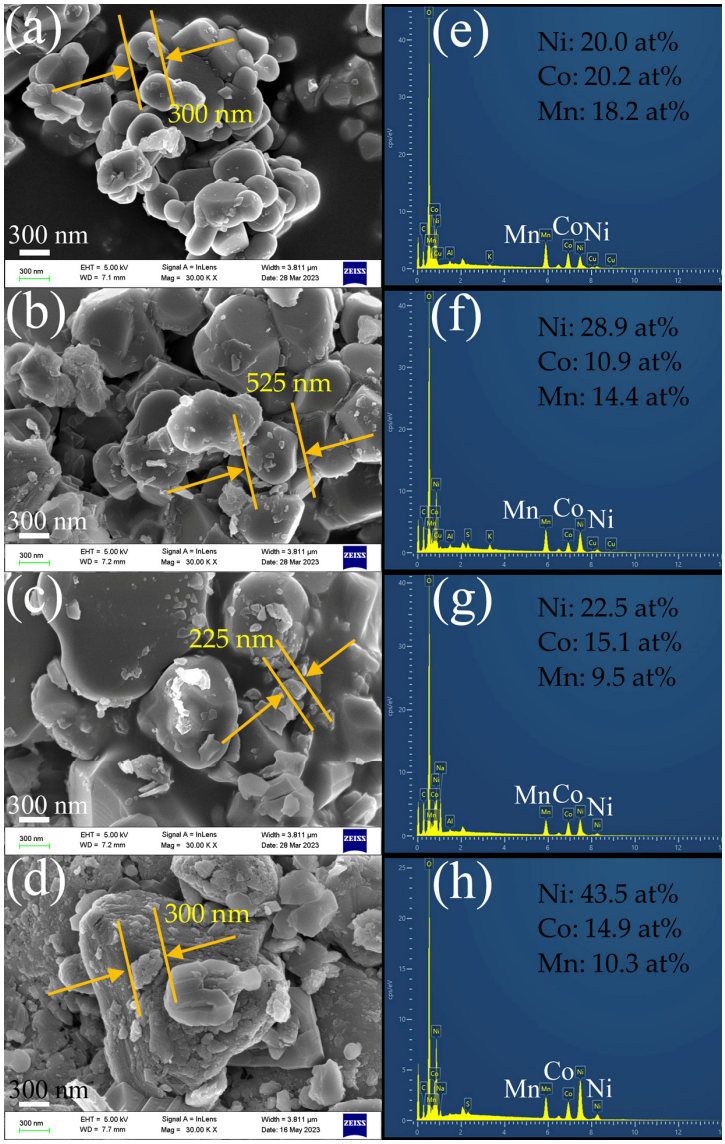

Figure 2. SEM images of regenerated NCM: (**a**) R333, (**b**) R523, (**c**) R532, and (**d**) R622 (Scale bar: 300 nm), and (**e**–**h**) corresponding EDS spectra with composition (insect table).

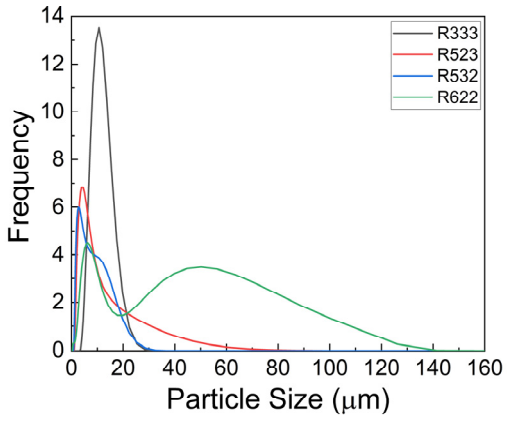

Figure 3. Frequency curve of the regenerated NCM powders' PSD (D_{90}) after Li scintering.

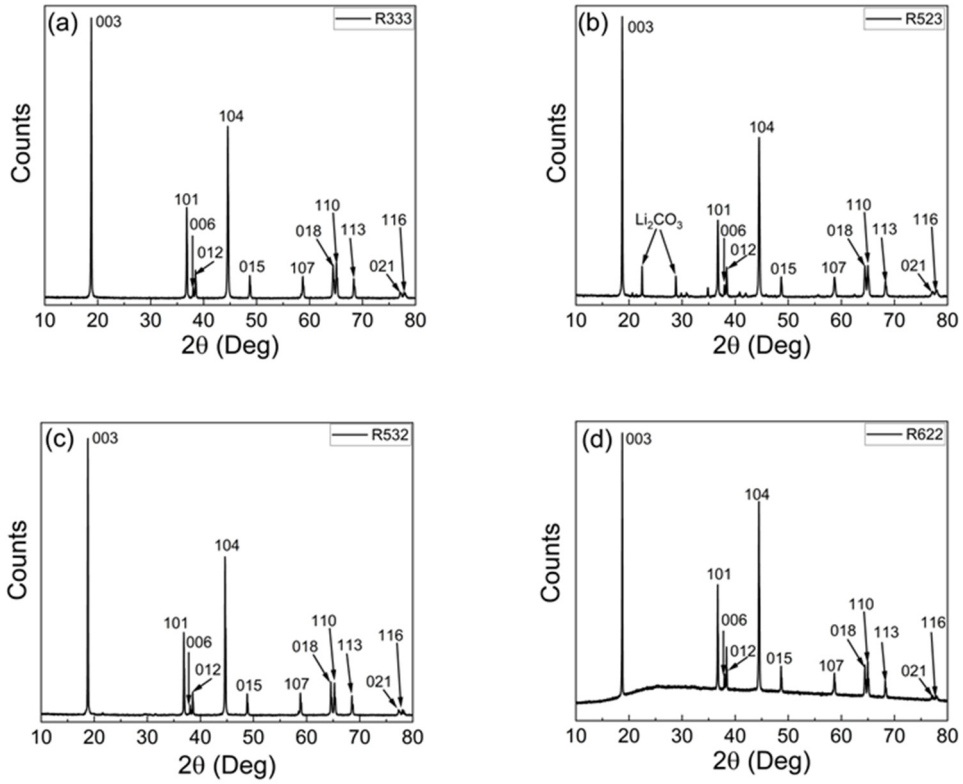

Figure 4. XRD pattern of regenerated NCMs: (**a**) R333, (**b**) R523, (**c**) R532, and (**d**) R622.

Elemental information of regenerated NCM black powder with different NCM combinations was analyzed by XPS, with the results generalized in Figures 5 and S3. Survey spectra (Figures 5a,b and S3a,b) showed that Ni, Co, and Mn were major components in the regenerated NCM. In-depth analysis by the HR-XPS (Figures 5c–j and S3c–j) showed the presence of the metallic 2p3/2 (Ni: 854.38–855.78 eV; Co: 779.68–780.18 eV; Mn: 641.98–642.68 eV) and 2p1/2 (Ni: 872.58–873.08 eV; Co: 795.08–795.58 eV; Mn: 653.18–654.18 eV) peaks with corresponding satellite peaks next to the above-mentioned main peaks (Ni: 860.88–861.28 eV (2p3/2), 878.38–879.88 eV (2p1/2); Co: 789.68–790.48 eV) in three individual metals (Ni (Figures 5c,d and S3c,d), Co (Figures 5e,f and S3e,f), Mn (Figures 5g,h and S3g,h)). Such findings show that Ni and Co existed in the form of NiO and Co_3O_4 by comparing these results with similar reported samples [21–23,25,26]. While the shoulder peak observed in Co2p3/2 (773–778 eV, Figures 5 e,f and S3e,f) and Mn2p3/2 (637.18–637.98 eV, Figures 5g,h and S3g,h) represented the Ni-Auger peak in the Mn and Co part of the NCM samples, such a signal did not affect the 2p1/2 peaks position of Co and Mn. It was similar to the pristine NCM samples reported elsewhere [25]. At the same time, a relatively weak Li1s peak was observed at 53.98–54.78 eV in regenerated NCM samples (Survey spectra: Figures 5a,b and S3a,b, HR-XPS Li1s: Figures 5i,j and S3i,j), which reflected the presence of metallic Li [22] after the Li_2CO_3 scintering with a co-precipitated NCM hydroxide precursor at 900 °C. This represented the co-existence of the ternary NCM oxide with metallic Li after lithiation.

In summary, by combining the results from elemental (EDS, ICP-MS, XPS), crystal (XRD), and micronanostructure (SEM) analysis (Figures 2–5 and Table 1), tailorable NCM regeneration into various designated NCM ratios from a mixture of spent LIB black powder via an environmentally friendly process (biodegradable strong acid, room temperature) was achieved in the current study.

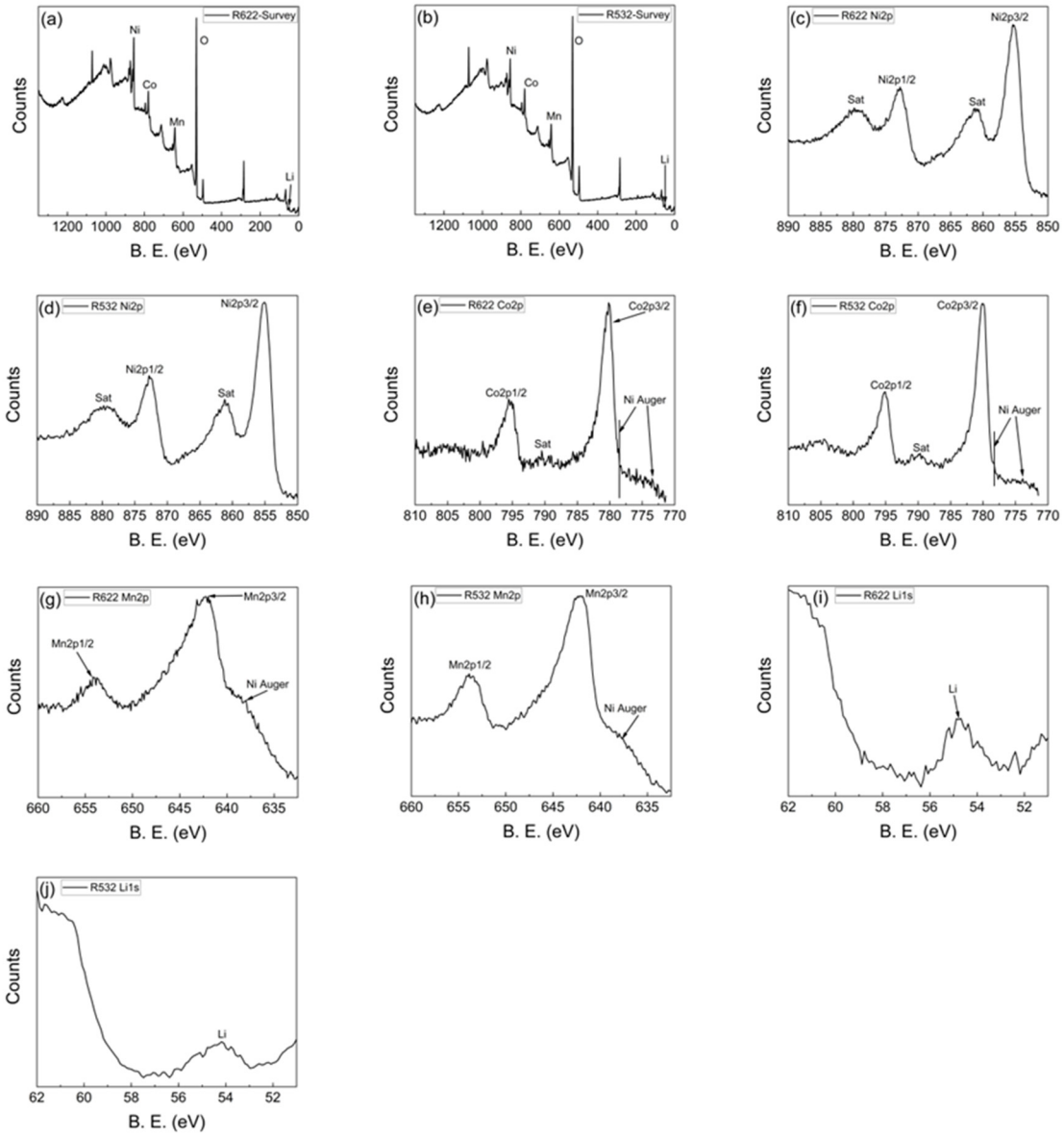

Figure 5. XPS pattern of regenerated NCM with different ratios. Survey spectrum: (**a**) R622, (**b**) R532, and HRXPS spectra: Ni2p of (**c**) R622, (**d**) R532; Co2p of (**e**) R622, (**f**) R532; Mn2p of (**g**) R622, (**h**) R532; and Li1s of (**i**) R622, (**j**) R532.

3.2. Battery Performance Testing

The electrochemical properties of regenerated NCM were evaluated in a CR2032 coin cell test in room temperature in order to explore the potential application of a second-life battery. They were determined by the cycling performance and galvanostatic charging-discharging profile, which are summarized in Figures 6 and 7 respectively. In the activation cycle (first cycle), initial capacity, discharging capacity, and columbic efficiency in descending order were R622 (181.1 mAh/g) > R532 (144.0 mAh/g) > R523 (131.7 mAh/g) > R333 (127.3 mAh/g) and R333 (90.51%) > R532 (84.60%) > R622 (80.98%) > R523 (79.04%), respectively. However, in practice, the actual performance study was counted from the second cycle of operation due to natural coin cell warming up in the first operational cycle. All regenerated NCM cathode-equipped CR2032 coin battery samples showed stable charging/discharging properties, as all samples showed a high columbic efficiency percentage of ~100%, which was recorded from the 2nd to the 51st cycle of the performance test (Figure 6). The cycling performance test at a scan rate of 0.1 C and with an applied voltage window of

3.0–4.2 V vs. Li^+/Li illustrated in Figure 6 shows the maximum specific discharging capacity at cycle 2 (first cycle after battery startup) in descending order of R622 (196.6 mAh/g) > R532 (152.0 mAh/g) > R333 (139.0 mAh/g) > R523 (136.3 mAh/g). After 51 cycles of operation, specific discharge capacity in descending order became R622 (144.6 mAh/g) > R532 (118.2 mAh/g) > R333 (117.9 mAh/g) > R523 (90.2 mAh/g). This tendency was also reflected from the discharge curves in the charging-discharging profile illustrated in Figure 7. Comparison of two plots showed that the discharge capacity depreciation percentage in decending order was R523 (33.9%) > R622 (26.7%) > R532 (22.2%) > R333 (15.3%). R333 showed the lowest discharge capacity depreciation (15.3%) among the four samples (Figures 6a and 7a). In contrast, the battery performance of R523 and R532 was the worst of the four in terms of discharge capacity (Figure 6b,c) and estimated capacity depreciation percentage. The discharge capacity depreciation percentage of R622 recorded at the 51st cycle lay between that of R523 and R532. Even though the deprciation percentage of R333 was the lowest, the recorded discharge capacity of R333 at the 51st cycle was smaller than that of R622 (Figures 6d and 7d). In general, even though the discharge capacity depreciation percentage of R622 was higher than that of R333, R622 is still regarded as the best battery among all candidates based on the discharge capacity described previously (Figure 7).

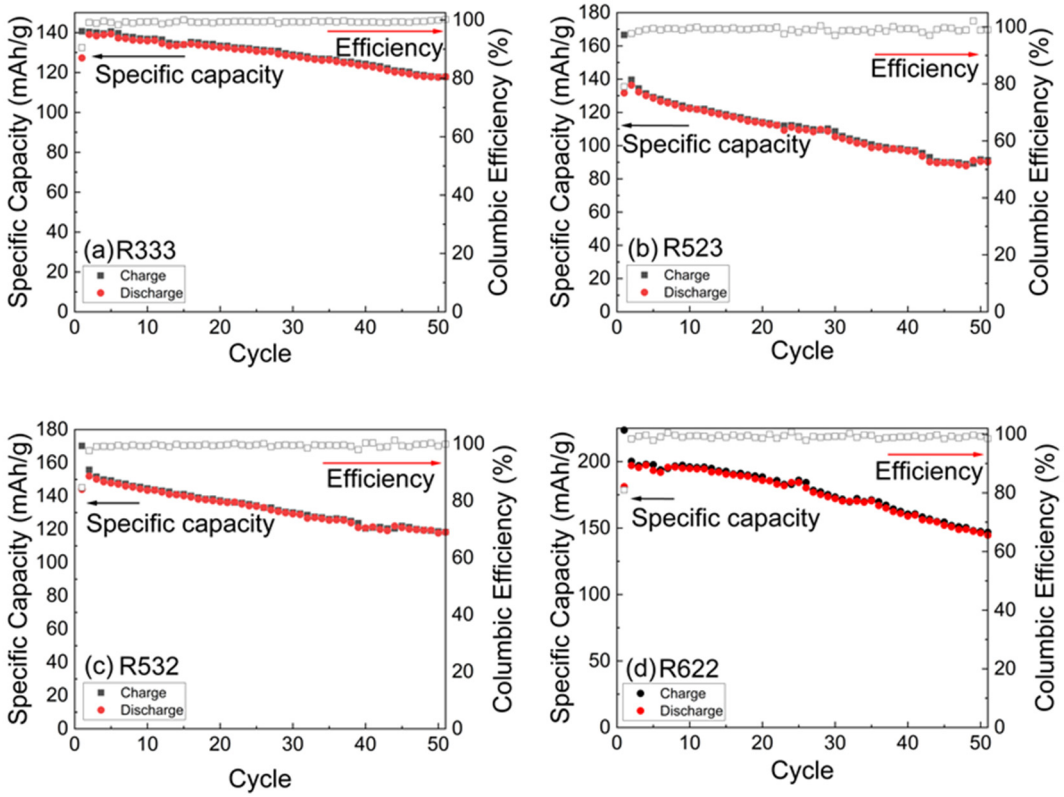

Figure 6. Cycling profile of (**a**) R333, (**b**) R523, (**c**) R532, and (**d**) R622 CR2032 battery in the first 50 cycles at 0.1 C scan rate.

Since high Ni content ternary NCM LIBs are popular for high-performance devices, R622 had the highest Ni content and the highest performance of the four regenerated NCM-equipped coin batteries (Figures 6 and 7). So, R622 was chosen for comparison with regenerated NCM cathode performance, which was synthesized by similar methods reported elsewhere. From the results summarized in Table 2, regenerated NCM R622 used in the current work has comparable cathode performance to reported regenerated NCM. It also showed that the regenerated NCM has satisfactory half-cell (Li block anode) performance, which provides the potential of commercialization of second-life NCM LIB production via mild and green conditioned NCM regeneration. Some reports have claimed

that large secondary particle sizes resulted from the multiple aggregation of NCM particles throughout regeneration and this may have had an impact on their cycling performance. Larger particle size may enhance charging/discharging activity due to an increase in a particle's tap density [21], even though the NCM ratio is the same [3,5,9,21]. Results summarized in Tables 1 and 2, and Figures 6 and 7 indicate that particle size (Figures 2 and 3) [3,5,9,21], and the presence of the Li_2CO_3 impurities in the R523 (XRD spectrum in Figure 4b) may affect the cycling performance of regenerated NCM samples. On the other hand, the mass loading of regenerated NCM in cathodes being used in this work (~1.1–1.6 mg/cm^2, Table 2) was relatively lower than some of regenerated NCM products (~1.8–20 mg/cm^2) with the same NCM ratio (including 333, 523, 532 and 622) [3–5,11,12,15,21], which shows that the R622 coin battery activity achieved in this work is comparable to a reported one [12]. Further in-depth investigation on the effect of crystalline structure and mass loading on a second-life battery can be expected to improve the activity of regenerated NCM produced from the mixture of spent NCM LIBs.

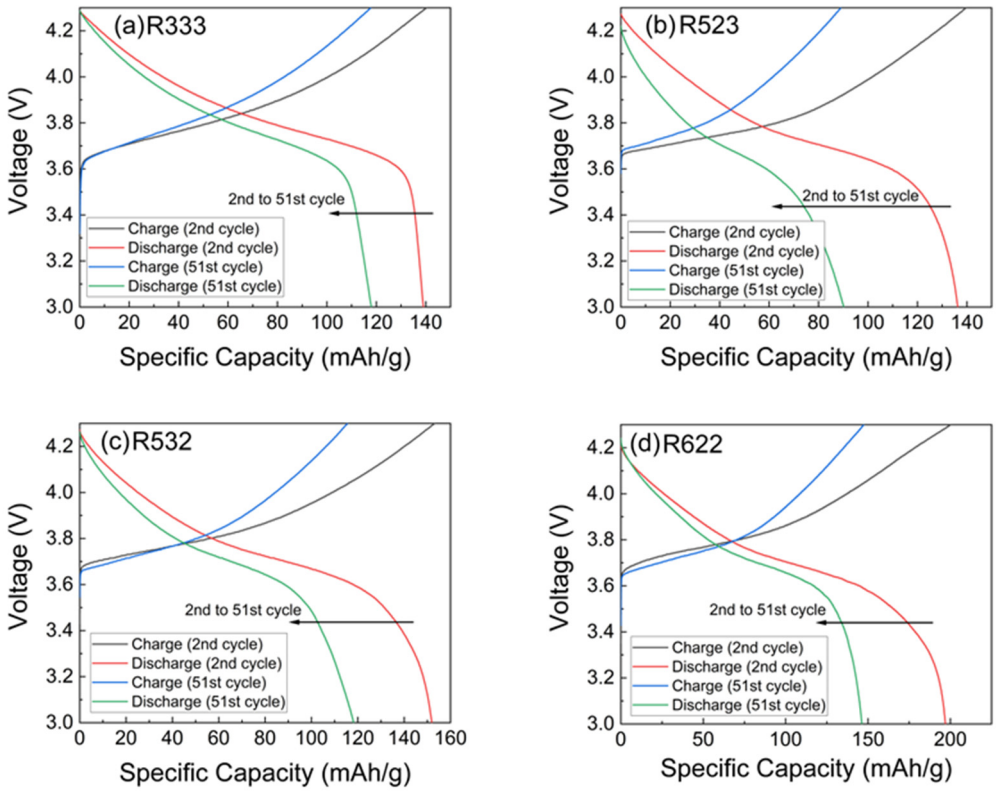

Figure 7. Charging/discharging profile of regenerated NCM coin battery: (**a**) R333, (**b**) R523, (**c**) R532, and (**d**) R622 (2nd vs. 51st cycle).

Table 2. Survey of cathode performance of regenerated 622 (discharge capacity at final recorded cycle as listed in retention column).

NCM	Sample Name	Discharge Capacity (mAh/g)	Retention %	Ref
622	R-NCM	144.5	86	[2]
622	R-NCM60	162.5	90.7	[12]
622	R-NCM30	135.4	88.3	[12]
622	R622	144.6	73.4	This work

Currently, most regenerated NCM involves the use of strong mineral acid (e.g., H_2SO_4) [1,2,9,11,14–16,19] for metal recovery, which can lead to secondary pollution by

the sulphur dioxide (SO_2), chlorine (Cl_2), or nitrous oxide (N_xO_y) produced. Weak organic acid ($pK_a > 0$, e.g., oxalic acid)-assisted leaching [12] carries a risk of low metal recovery efficiency. In contrast, the PTA used in the current work showed comparable activity to strong mineral acid ($pK_a < 0$)-assisted recovery with the advantage of being cost-effective [27]. Furthermore, the targeted tailoring of the NCM ratio was fixed at a single value for most of study, regardless of whether it was recovered from single or multiple spent LIBs [2–5,9,11,12,14–19]. Furthermore, some NCM regeneration with a tailored ratio via the co-precipitation process was carried out in an inert gas environment (N_2 [5,21], Ar [9,14]) with heating [9,21]. NCM regeneration by tailoring to the designated NCM ratio was achieved in room temperature and ambient atmosphere in the current work, which shows that spent LIBs could be recycled, as different types of spent LIBs could be collected together from customers, and there is potential for commercialization of second-life NCM LIB production under mild and less pollutive conditions. It is important for promoting sustainable LIB manufacturing in order to achieve a circular economy of energy storage materials (metal resources). In addition, life-cycle assessment (LCA) of NCM regeneration (PTA-assisted hydrometallurgy of spent NCM black powder mixture leaching and co-precipitation into regenerated NCM) and further improvement of the hydrometallurgy and regeneration processes can be expected to optimize these processes to achieve the best NCM regeneration, and solve the problem of random activity of regenerated NCM samples caused by random particle size formed in the final product after the co-precipitation step.

4. Conclusions

In summary, under mild conditions, tailorable NCM ratio regeneration from mixed spent LIB cathode black powder by strong organic acid (PTA)-assisted leaching and metal ion co-precipitation was achieved in this study. The NCM ratio achieved in the regenerated NCM was close to the designated value in the metal ion content adjustment step. Regenerated NCM black powders also exhibited highly crystalline structure and the presence of metallic Li. Furthermore, the regenerated NCM (R622) CR2032 coin cell (Li anode half-cell) exhibited high performance in charge/discharge cycling testing, with low activity depreciation. This provides the possibility of industrial-scale, multiple-waste LIBs recycling into second-life LIBs with a tailorable NCM ratio. It is important for the development of sustainable LIB manufacturing for a circular economy in future.

Supplementary Materials: The following supporting information can be downloaded at https://www.mdpi.com/article/10.3390/electrochem5040035/s1, Figure S1: Pre-treatment of waste LIBs. (a) Brine solution discharge, (b) and (c) manual scraping, (d) dried cathode sheets after scraping and DI water washing via overnight drying; Figure S2: Extraction process of NCM metals from cathode powder. (a) Cathode sheet cutting, (b) cathode sheet calcination at 600 °C in air, (c) peel-off of cathode powder manually, (d) organic acid (PTA) leaching at low temperature (40 °C), (e) leachate collection for regeneration after filtering; Figure S3. XPS pattern of regenerated NCM with different ratio. Survey spectrum: (a) R333, (b) R523, and HRXPS spectra: Ni2p of (c) R333, (d) R523; Co2p of (e) R333, (f) R523; Mn2p of (g) R333, (h) R523; and Li1s of (i) R333, (j) R523; Table S1: Metal composition in the raw leachates (ICP) vs. raw powder (EDS), and that of leachate stock (ICP) for NCM regeneration; Table S2: Mass loading of the regenerated cathodes.

Author Contributions: Conceptualization, A.C.H.T. and X.-Y.L.; methodology, A.C.H.T.; validation, X.-Y.L. and A.C.H.T.; formal analysis, A.C.H.T.; investigation, X.-Y.L. and A.C.H.T.; resources, S.O., Y.L., C.C.L., C.-W.T. and X.-Y.L.; data curation, A.C.H.T. and X.-Y.L.; writing—original draft preparation, A.C.H.T.; writing—review and editing, C.-W.T. and X.-Y.L.; supervision, X.-Y.L.; project administration, X.-Y.L.; funding acquisition, X.-Y.L. All authors have read and agreed to the published version of the manuscript.

Funding: This research was funded by The Research Matching Grant Scheme (RMG/036 and RMG/039) of UGC-HK.

Institutional Review Board Statement: Not applicable.

Informed Consent Statement: Not applicable.

Data Availability Statement: The data presented in this study are available on request from the corresponding author.

Acknowledgments: SEM images and EDS spectra of regenerated NCM was acquired at Institute of Advanced Materials, Hong Kong Baptist University.

Conflicts of Interest: The authors declare no conflicts of interest.

References

1. Liu, P.C.; Yang, X.R.; Xiao, L.; Chen, H.; Chen, H. Preparation of Ternary Precursor Derived from Spent $LiNi_xCo_yMn_{1-x-y}O_2$ Materials. *JOM* **2019**, *71*, 4492–4499. [CrossRef]
2. Shang, M.; Peng, L.X. The regeneration and electrochemical performance study of NCM622 cathode materials. *Ionics* . [CrossRef]
3. Shi, Y.; Chen, G.; Liu, F.; Yue, X.J.; Chen, Z. Resolving the Compositional and Structural Defects of Degraded $LiNi_xCo_yMn_zO_2$ Particles to Directly Regenerate High-Performance Lithium-Ion Battery Cathodes. *ACS Energy Lett.* **2018**, *3*, 1683–1692. [CrossRef]
4. Fan, X.P.; Tan, C.L.; Li, Y.; Chen, Z.Q.; Li, Y.H.; Huang, Y.G.; Pan, Q.C.; Zheng, F.H.; Wang, H.Q.; Li, Q.Y. A green, efficient, closed-loop direct regeneration technology for reconstructing of the $LiNi_{0.5}Co_{0.2}Mn_{0.3}O_2$ cathode material from spent lithium-ion batteries. *J. Hazard. Mater.* **2021**, *410*, 124610. [CrossRef] [PubMed]
5. Ma, X.T.; Chen, M.Y.; Zheng, Z.F.; Bullen, D.; Wang, J.; Harrison, C.; Gratz, E.; Lin, Y.L.; Yang, Z.Z.; Zhang, Y.T.; et al. Recycled cathode materials enabled superior performance for lithium-ion batteries. *Joule* **2021**, *5*, 2955–2970. [CrossRef]
6. Fan, M.; Chang, X.; Meng, Q.; Wan, L.-J.; Guo, Y.-G. Progress in the sustainable recycling of spent lithium-ion batteries. *SusMat* **2021**, *1*, 241–254. [CrossRef]
7. Du, K.D.; Ang, E.H.; Wu, X.L.; Liu, Y.C. Progresses in Sustainable Recycling Technology of Spent Lithium-Ion Batteries. *Energy Environ. Mater.* **2022**, *5*, 1012–1036. [CrossRef]
8. Sun, Y.; Yang, H.; Li, J.; Li, J.; Zhuge, X.; Ren, Y.; Ding, Z. A large volume and low energy consumption recycling strategy for $LiNi_{0.6}Co_{0.2}Mn_{0.2}O_2$ from spent ternary lithium-ion batteries. *J. Power Sources* **2024**, *602*, 234407. [CrossRef]
9. Xing, L.; Lin, S.; Yu, J.G. Novel Recycling Approach to Regenerate a $LiNi_{0.6}Co_{0.2}Mn_{0.2}O_2$ Cathode Material from Spent Lithium-Ion Batteries. *Ind. Eng. Chem. Res.* **2021**, *60*, 10303–10311. [CrossRef]
10. Song, D.; Yu, J.; Wang, M.; Tan, Q.; Liu, K.; Li, J. Advancing recycling of spent lithium-ion batteries: From green chemistry to circular economy. *Energy Storage Mater.* **2023**, *61*, 102870. [CrossRef]
11. Chen, X.Q.; Yang, C.F.; Yang, Y.B.; Ji, H.M.; Yang, G. Co-precipitation preparation of Ni-Co-Mn ternary cathode materials by using the sources extracting directly from spent lithium-ion batteries. *J. Alloy. Compd.* **2022**, *909*, 164691. [CrossRef]
12. Huang, Z.X.; Liu, X.; Zheng, Y.; Wang, Q.; Liu, J.W.; Xu, S.M. Boosting efficient and low-energy solid phase regeneration for single crystal $LiNi_{0.6}Co_{0.2}Mn_{0.2}O_2$ via highly selective leaching and its industrial application. *Chem. Eng. J.* **2023**, *451*, 139039. [CrossRef]
13. Baars, J.; Domenech, T.; Bleischwitz, R.; Melin, H.E.; Heidrich, O. Circular economy strategies for electric vehicle batteries reduce reliance on raw materials. *Nat. Sustain.* **2021**, *4*, 71–79. [CrossRef]
14. Wang, G.G.; Wu, T.; Liu, B.R.; Gong, S.S.; Huang, Q.; Su, Y.F.; Wu, F.; Kelly, R.M. Gradient-Regeneration of $Li(Ni_{0.9}Co_{0.05}Mn_{0.05})O_2$ from Spent $LiCoO_2$ lithium-Ion Battery. *J. Electrochem. Soc.* **2020**, *167*, 160557. [CrossRef]
15. Shi, Y.; Zhang, M.H.; Meng, Y.S.; Chen, Z. Ambient-Pressure Relithiation of Degraded $Li_xNi_{0.5}Co_{0.2}Mn_{0.3}O_2$ (0<x<1) via Eutectic Solutions for Direct Regeneration of Lithium-Ion Battery Cathodes. *Adv. Energy Mater.* **2019**, *9*, 1900454.
16. Zhou, H.M.; Zhao, X.X.; Yin, C.J.; Li, J. Regeneration of $LiNi_{0.5}Co_{0.2}Mn_{0.3}O_2$ cathode material from spent lithium-ion batteries. *Electrochim. Acta* **2018**, *291*, 142–150. [CrossRef]
17. Jiang, G.H.; Zhang, Y.N.; Meng, Q.; Zhang, Y.J.; Dong, P.; Zhang, M.Y.; Yang, X. Direct Regeneration of $LiNi_{0.5}Co_{0.2}Mn_{0.3}O_2$ Cathode from Spent Lithium-Ion Batteries by the Molten Salts Method. *ACS Sustain. Chem. Eng.* **2020**, *8*, 18138–18147. [CrossRef]
18. Chen, X.Q.; Feng, Y.Y.; Zhang, S.; Kou, W.Z.; Ji, H.M.; Yang, G. Comparison study on regeneration of spent ternary materials by molten salt solid-liquid method and traditional solid-solid method. *J. Alloy. Compd.* **2022**, *900*, 163308. [CrossRef]
19. Tang, X.D.; Guo, Q.K.; Zhou, M.M.; Zhong, S.W. Direct regeneration of $LiNi_{0.5}Co_{0.2}Mn_{0.3}O_2$ cathode material from spent lithium-ion batteries. *Chin. J. Chem. Eng.* **2021**, *40*, 278–286. [CrossRef]
20. Wang, B.; Lin, X.Y.; Tang, Y.Y.; Wang, Q.; Leung, M.K.H.; Lu, X.Y. Recycling $LiCoO_2$ with methanesulfonic acid for regeneration of lithium-ion battery electrode materials. *J. Power Sources* **2019**, *436*, 226828. [CrossRef]
21. Mugumya, J.H.; Rasche, M.L.; Rafferty, R.F.; Patel, A.; Mallick, S.; Mou, M.Y.; Bobb, J.A.; Gupta, R.B.; Jiang, M. Synthesis and Theoretical Modeling of Suitable Co-precipitation Conditions for Producing NMC111 Cathode Material for Lithium-Ion Batteries. *Energy Fuels* **2022**, *36*, 12261–12270. [CrossRef]
22. Wood, K.N.; Teeter, G. XPS on Li-Battery-Related Compounds: Analysis of Inorganic SEI Phases and a Methodology for Charge Correction. *ACS Appl. Energ. Mater.* **2018**, *1*, 4493–4504. [CrossRef]
23. Wang, L.Z.; Zhang, J.H.; Fang, H.; Gao, K.Z.; Yan, J. $LiNi_{0.8}Co_{0.1}Mn_{0.1}O_2/Li_xCoO_2$ hybrid cathode and Its Enhanced Electrochemical Properties for Lithium Ion Batteries Lithium Ion Batteries. *Int. J. Electrochem. Sci.* **2020**, *15*, 11684–11699. [CrossRef]
24. Zhang, L.L.; Wang, J.Q.; Yang, X.L.; Liang, G.; Li, T.; Yu, P.L.; Ma, D. Enhanced Electrochemical Performance of Fast Ionic Conductor $LiTi_2(PO_4)_3$-Coated $LiNi_{1/3}Co_{1/3}Mn_{1/3}O_2$ Cathode Material. *ACS Appl. Mater. Interfaces* **2018**, *10*, 11663–11670. [CrossRef]

25. Bondarchuk, O.; LaGrow, A.P.; Kvasha, A.; Thieu, T.; Ayerbe, E.; Urdampilleta, I. On the X-ray photoelectron spectroscopy analysis of $LiNi_xMn_yCo_zO_2$ material and electrodes. *Appl. Surf. Sci.* **2021**, *535*, 147699. [CrossRef]
26. Su, X.; Wang, X.P.; Bareno, J.; Qin, Y.; Aguesse, F.; Lu, W.Q. Enable High-Energy $LiNi_{0.5}Co_{0.2}Mn_{0.3}O_2$ by Ultra-Thin Coating through Wet Impregnation. *Batteries* **2022**, *8*, 136. [CrossRef]
27. Liu, J.; Mak, T.Y.; Meng, Z.; Wang, X.; Cao, Y.; Lu, Z.; Suen, D.W.-S.; Lu, X.-Y.; Tang, Y. Efficient recovery of lithium as Li_2CO_3 and cobalt as Co_3O_4 from spent lithium-ion batteries after leaching with p-toluene sulfonic acid. *Hydrometallurgy* **2023**, *216*, 106012. [CrossRef]